Antiproliferative Effects of Pomegranate Extract in MCF-7 Breast Cancer Cells are Associated with Reduced DNA Repair Gene Expression and Induction of Double Strand Breaks

Amit B. Shirode,[1,2,†] Prasad Kovvuru,[1,2,†] Sridar V. Chittur,[2,3] Susanne M. Henning,[4] David Heber,[4] and Ramune Reliene[1,2]*

[1]*Department of Environmental Health Sciences, University at Albany, State University of New York, Albany, New York*
[2]*Cancer Research Center, University at Albany, Rensselaer, New York*
[3]*Department of Biomedical Sciences, University at Albany, State University of New York, Albany, New York*
[4]*Center for Human Nutrition, David Geffen School of Medicine, University of California, Los Angeles, California*

Pomegranate extract (PE) inhibits the proliferation of breast cancer cells and stimulates apoptosis in MCF-7 breast cancer cells. While PE is a potent antioxidant, the present studies were conducted to examine the mechanisms of action of PE beyond antioxidation by studying cellular and molecular mechanisms underlying breast tumorigenesis. PE inhibited cell growth by inducing cell cycle arrest in G_2/M followed by the induction of apoptosis. In contrast, antioxidants *N*-acetylcysteine and Trolox did not affect cell growth at doses containing equivalent antioxidant capacity as PE, suggesting that growth inhibition by PE cannot solely be attributed to its high antioxidant potential. DNA microarray analysis revealed that PE downregulated genes associated with mitosis, chromosome organization, RNA processing, DNA replication and DNA repair, and upregulated genes involved in regulation of apoptosis and cell proliferation. Both microarray and quantitative RT-PCR indicated that PE downregulated important genes involved in DNA double strand break (DSB) repair by homologous recombination (HR), such as *MRE11*, *RAD50*, *NBS1*, *RAD51*, *BRCA1*, *BRCA2*, and *BRCC3*. Downregulation of HR genes correlated with increased levels of their predicted microRNAs (miRNAs), miR-183 (predicted target RAD50) and miR-24 (predicted target BRCA1), suggesting that PE may regulate miRNAs involved in DNA repair processes. Further, PE treatment increased the frequency of DSBs. These data suggest that PE downregulates HR which sensitizes cells to DSBs, growth inhibition and apoptosis. Because HR represents a novel target for cancer therapy, downregulation of HR by PE may be exploited for sensitization of tumors to anticancer drugs.

Key words: pomegranate extract; breast cancer; homologous recombination; DNA repair

INTRODUCTION

Pomegranate is consumed as whole fruit and also widely available commercially as fruit juice, wine, or sauce [1]. The fruit can be divided into three parts: the seeds, the juice, and the peel. Extracts of all parts of the fruit appear to have therapeutic properties. Pomegranate fruit is a rich source of many phenolic compounds including flavonoids (anthocyanins, catechins, and other complex flavonoids) and hydrolyzable tannins called ellagitannins (punicalin, pedunculagin, punicalagin, gallagic, and ellagic acid esters of glucose) [2]. The concentration of total polyphenols in pomegranate juice (3.8 mg/mL gallic acid equivalents) is higher than other fruit juices (grape, blueberry, black cherry, cranberry, orange, apple, which contain only 0.4–2.6 mg/mL of gallic acid equivalents) [3]. In turn, pomegranate juice has the highest antioxidant capacity as compared to other polyphenol-rich beverages, such as red wine, grape juice, blueberry juice, and green tea [3]. The potent antioxidant properties of pomegranate juice have been thought to be responsible for various health benefits. However, it has not been established whether antioxidant effects per se can explain the actions of pomegranate juice in inhibiting tumor cell growth in vitro.

The effects of pomegranate extract (PE) containing primarily ellagitannins have been evaluated in vitro in terms of antiproliferative, antiinvasive, and proapoptotic properties in several different cancer cell lines [4–7]. Pomegranate juice as a whole has

Additional supporting information may be found in the online version of this article.

Abbreviations: PE, pomegranate extract; NAC, N-acetylcysteine; miRNA, microRNA; TEAC, Trolox equivalent antioxidant capacity; TE, Trolox equivalent; MRN, MRE11–RAD50–NBS1 complex; DSB, double strand break; HR, homologous recombination; NHEJ, nonhomologous end joining.

[†]Amit B. Shirode and Prasad Kovvuru contributed equally to this work.

*Correspondence to: 1 Discovery Drive, Cancer Research Center Rm. 304, Rensselaer, NY 12144.

Received 25 October 2012; Revised 6 December 2012; Accepted 8 December 2012

DOI 10.1002/mc.21995

Published online in Wiley Online Library (wileyonlinelibrary.com).

been found to be more effective as compared to isolated phytochemicals given individually [8]. Although the main focus of research has been on prostate cancer, the anticancer potential of pomegranate has also been examined in breast cancer albeit only in in vitro studies [9–12]. Different PE preparations reduced growth of both estrogen-receptor positive as well as estrogen-receptor negative breast cancer cell lines [10], mammary organ culture [9], MMTV-Wnt-1 mouse mammary cancer stem cells [13] and reduced the motility and invasion of MDA-231 and SUM 149 cell lines derived from aggressive tumors [12]. The observed effects were associated with inhibition of NF-κB expression [12] and/or inhibition of 17β-hydroxysteroid dehydrogenase (aromatase), the enzyme that catalyzes conversion of estrone to estradiol [11]. Estradiol has been suggested to increase the risk of breast cancer in postmenopausal women leading to recommendations that dietary interventions that reduce estrogen synthesis may be beneficial for cancer prevention [14]. In summary, these studies suggested that pomegranate intake can modulate tumor behavior by reducing growth and/or invasiveness as well as suppressing hormonal carcinogenesis through reduction of estrogen levels and/or activity.

While the beneficial properties of pomegranate are being investigated, the studies of its adverse effects have not been neglected either. Subchronic toxicity study in rats showed that oral administration of PE at 600 mg/kg/d, the highest dose tested, for 90 d is devoid of any significant adverse effects based on clinical observations, ophthalmic examination, body weights, body weight gains, feed consumption, clinical pathology evaluations, organ weights, hematological and serum chemistry parameters and gross and histopathology analysis after terminal necropsy [15].

The antioxidant capacity of pomegranate ellagitannins has been proposed to account for their pharmacological actions, although the link between antioxidant capacity and tumor growth inhibition has not been established. The genome-wide transcriptome analysis of PE effects in breast cancer cells has not been reported to date. In the present study, an integrative approach was applied using Affymetrix gene arrays to identify changes in gene expression following treatment with PE in MCF-7 breast cancer cells and then validating relative mRNA expression by quantitative RT-PCR (qRT-PCR). In addition, further analysis of the expression of predicted microRNAs (miRNAs) for significantly modulated genes was carried out. To assess whether the antioxidant effects of PE could explain the observed growth inhibition of breast cancer cells, cells were exposed to typical antioxidants, *N*-acetylcysteine (NAC) and Trolox.

MATERIALS AND METHODS

Pomegranate Extract

PE is a standardized extract (POMX, POM Wonderful, Los Angeles, CA) of pomegranate fruit grown in California (*Punica granatum L.*, Wonderful variety; Paramount Farms, Lost Hills, CA). PE is made from fruit skins and consists of 95% glycone ellagitannins (mono and oligomeric) standardized to punicalagins (37–40%) and free ellagic acid (3.4%) as determined by high-performance liquid chromatography using previously described methods [16].

Cell Line, Culture Conditions, and Experimental Treatments

MCF-7 cells (a gift from Dr. Welsh lab, Cancer Research Center, University at Albany, State University of New York) were grown and maintained in Minimum Essential Medium Eagle (Sigma-Aldrich, St. Louis, MO) supplemented with 25 mM HEPES (Fisher Scientific, Fair Lawn, NJ), 20 mM D-(+)glucose, 100 U/mL penicillin and 100 μg/mL streptomycin and 5% fetal bovine serum (Sigma-Aldrich). Cells were maintained at 37.0°C in a humidified atmosphere of 95.0% air and 5.0% CO_2. Stock solution of PE (1 mg/mL) was prepared in ddH_2O. Stock solution of Trolox (Sigma-Aldrich) (0.5 mM) was prepared by dissolving 6.26 mg Trolox in 50 mL Na/K buffer and slightly warming the solution further (30°C in water bath). Three hundred micromolar working stock solution of NAC (Sigma-Aldrich) was prepared by serial dilution from a 30 mM stock in ddH_2O. These stock solutions were then used to prepare various concentrations of drug-supplemented treatment media. MCF-7 cells were initially plated at a density of 2×10^4 cells/well (3 wells/group) in a volume of 1 mL/well of culture medium in 24-well plates. Cells were allowed to adhere for 24 h. The following day, cells were divided into different treatment groups. Media was removed and replaced with fresh control or treatment media. Cells were treated with increasing doses of PE (0–100 μg/mL), NAC (0–40 μg/mL), or Trolox (0–75 μg/mL) for a period of 72 or 96 h. For 96 h treatments, cells in their respective treatment groups were fed fresh control or treatment media after 48 h. For 72 h treatments groups, control or treatment media were not changed. To assess the sustainability of growth inhibition cells were treated with 50 μg/mL of PE for 72 h followed by cell culturing in PE-free medium for additional 96 h.

Measurement of Viable Cell Number

The determination of cell viability was first tested by MTT (3-[4,5-dimethylthiazol-2-yl]-2,5-diphenyl tetrazolium bromide) assay. However, polyphenols have been shown to interfere with the redox chemistry of MTT assay system leading to false positive responses [17]. Consistent with these observations, PE itself was found to generate colorimetric

responses in the absence of cells, possibly due to interference with PE polyphenols. Hence, the effects of PE on MCF-7 cells were assessed by two alternative independent cell viability assays, crystal violet assay and acid phosphatase assay. Crystal violet assay gives quantitative information about the relative density of adhering cells [18], whereas acid phosphatase assay measures viable cell numbers by quantification of cytosolic acid phosphatase activity [19].

In crystal violet assays, culture medium was removed from each well at the end of treatment period and cells were washed with 500 μL PBS. Cells were fixed with 0.1% glutaraldehyde (Fisher Scientific) in PBS for 20 min followed by staining with 0.1% crystal violet for 30 min. The crystal violet stain (Sigma-Aldrich) was solubilized in 1% Triton X-100 (Sigma-Aldrich) in ddH_2O for 30 min and the absorbance was read with Victor^{3}V 1420 Multi-Label Counter (PerkinElmer, Inc., Waltham, MA) at 590 nm. Three independent biological replicates were analyzed each in triplicate.

In acid phosphatase assays, the culture medium was removed at the end of the treatment period and each well was washed once with 200 μL PBS. Buffer containing 0.1 M sodium acetate (pH 5.0), 0.1% Triton X-100 and 5 mM *p*-nitrophenyl phosphate (Sigma-Aldrich) was added and plates were incubated at 37.0°C for 2 h. The reaction was stopped with the addition of 100 μL of 1 N NaOH. The absorbance was read with Victor^{3}V 1420 Multi-Label Counter (PerkinElmer, Inc.) at 405 nm. Three independent biological replicates were analyzed each in triplicate.

Trolox Assay

Trolox equivalent antioxidant capacity (TEAC) assay measures antioxidant strength based on Trolox (6-hydroxy-2,5,7,8-tetramethylchroman-2-carboxylic acid) (Sigma-Aldrich) antioxidant capacity and is measured in units called Trolox equivalents (TEs). Trolox is a hydrophilic vitamin E analog that lacks the phytyl tail and has enhanced antioxidant capacity due to its increased cell permeability. Due to the difficulties in measuring individual antioxidant components of a complex mixture, Trolox equivalency is used as a benchmark for the antioxidant capacity of such a mixture [20]. The TEAC assay is based on the suppression of the absorbance of radical cations of 2,2′-azinobis(3-ethylbenzothiazoline 6-sulfonate) (ABTS) (Sigma-Aldrich) by antioxidants in the test sample when ABTS incubates with a peroxidase (metmyoglobin) and H_2O_2. The assay was performed as previously described [21]. Briefly, ABTS radical cations were prepared by adding 80 mg of manganese dioxide to 20 mL of 5 mM aqueous stock solution of ABTS in 75 mM Na/K buffer, pH 7. Trolox was used as an antioxidant standard. A standard calibration curve was constructed for Trolox at 0, 50, 100, 150, 200, 250, and 300 μM concentrations. Samples of PE and NAC were serially diluted in Na/K buffer, added in triplicates in a 96-well plate and mixed with 200 μL of ABTS+ radical cation solution. Absorbance was read at 750 nm after 5 min in a Labsystems Multiscan MCC/340 microplate reader (Fisher Scientific). TEAC values were calculated from the Trolox standard curve and expressed as TEs (mM). Based on the assay results, doses of PE, Trolox and NAC that were equivalent in terms of TEs were used to treat MCF-7 cells to assess the comparative growth inhibition at 72 h. Three independent biological replicates were analyzed each in triplicate.

Flow Cytometry

For flow cytometry studies, MCF-7 cells were initially plated at a density of 2×10^4 cells/well in triplicates in a volume of 1 mL/well of culture medium in 24-well plates. Cells were allowed to adhere for 24 h. The following day, media was removed and replaced with PE-supplemented or PE-free medium. At the end of 24, 48, and 72 h incubation, cells were harvested by trypsinization, 3 wells were pooled together and prepared for flow cytometric analysis of Apo-BrDU and PI staining as per the protocol (Phoenix Flow Systems, San Diego, CA). Following trypsinization, cells were fixed with 4% formaldehyde in PBS for 30 min on ice followed by 70% ethanol permeabilization overnight at −20°C. Samples were enzymatically labeled with bromodeoxyuridine triphosphate (BrdU) in TdT reaction buffer (2.5 mM cobalt chloride and 24 000 U terminal transferase) for 1 h at 37°C to label the 3′-OH ends of fragmented DNA (Roche Applied Science, Indianapolis, IN). DNA strand breaks were counterlabeled with FITC-conjugated anti-BrdU monoclonal antibody according to the manufacturer's recommendations (Phoenix Flow Systems). Cells were counterstained with 5 μg/mL propidium iodide (Sigma-Aldrich) in the presence of 0.015 U/mL RNase (Roche Applied Science) in PBS for 30 min at room temperature. Samples were analyzed on BD™ LSR II Flow Cytometer (BD Biosciences, San Jose, CA) within 1 h of labeling and a minimum of 10 000 events were analyzed for each experimental condition. Three independent biological replicates for each treatment group were analyzed.

Immunofluorescent Analysis of γ-H2AX Foci

Cells were propagated in 4-well Lab-Tek®II Chamber slides™ (NUNC A/S, Roskilde, Denmark) and treated with different doses of PE. At the end of each treatment period, cells were fixed with 4% paraformaldehyde, semi-permeabilized with 0.5% Triton-X 100 and washed with PBS as previously described [22]. Briefly, cells were incubated with 1:400 dilution of mouse monoclonal antibody to γ-H2AX (phosphorylated histone 2AX) (EMD Millipore, Billerica, MA), followed by 1:200 dilution of goat anti-mouse antibody to immunoglobulin labeled with

fluorescein isothiocyanate (FITC) (Jackson Immunochemicals, West Grove, PA) in PBS containing 10% FBS for 1.5 and 1 h, respectively, and mounted with Vectashield with 4′,6′-diamino-2-phenylindol (Vector Laboratories, Burlingame, CA). Cells were visualized at 100× using Nikon Eclipse TS100 microscope and analyzed for distinct nuclear foci. DAPI (1 μg/mL) in the mounting media was used as a counterstain. At least 100 cells were counted and cells with more than four distinct foci in the nucleus were considered positive for γ-H2AX. Three independent biological replicates were analyzed.

Microarray Profiling and Data Analysis

Total RNA was extracted by Trizol method according to the manufacturer instructions (Life Technologies, Ambion, Carlsbad, CA) from cells treated with 50 μg/mL of PE for 72 h and their respective controls, collected from three independent biological replicates at three different passage numbers. The quality of the RNA samples was assessed by NanoDrop 1000 Spectrophotometer (Thermo Fisher Scientific, Waltham, MA) and samples having 260/280 ratio ≈2.0 and 260/230 ratio ≈2.0 were selected. RNA integrity number (RIN) was measured for the treatment and control samples using Bioanalyzer (Agilent Technologies, Santa Clara, CA) and good quality samples (RIN $>$ 8) were further processed for hybridization into whole human genome Affymetrix Human Gene-1.0 ST array platform at the Center for Functional Genomics (Rensselaer, NY). All data were baseline transformed to the median of the control data. The data were filed to remove probesets with expression levels in the bottom 20th percentile across all samples. The entities were further processed through 1.5-fold filter settings to include those entities that were differentially expressed between PE treatments and controls. Differentially expressed entities were then passed to a *t*-test ($P < 0.05$) with a Benjamini-Hochberg False discovery rate correction to obtain the statistically significant and differentially expressed genes. DAVID functional annotation analysis was performed to highlight the most relevant gene ontology (GO)-term enrichment associated within the gene list. The downregulated/upregulated gene entities were then filtered by the default settings of EASE score threshold (Max. Prob $\leq$ 0.1 and Min. Count $\geq$ 2) to calculate the Fisher exact *P*-value for gene enrichment analysis (smaller the *P*-value, the stronger the enrichment in annotation categories).

In addition, we performed Ingenuity Pathway Analysis to identify molecular relationships among the genes that were differentially expressed in both microarrays and qRT-PCR.

qRT-PCR

Validation of the microarray data of selected genes was performed in MCF-7 cells treated with 50 μg/mL of PE for 24, 48, and 72 h on samples from biological experiments independent from those used for microarray analysis. Total RNA was isolated using Trizol and purified using NucleoSpin kit (Qiagen, Germantown, MD). The purity of the RNA was assessed by NanoDrop 1000 Spectrophotometer (Thermo Fisher Scientific). cDNA was synthesized from 1 μg of total RNA using Multiscribe reverse transcriptase enzyme (Applied Biosciences, Foster City, CA) and qRT-PCR was performed using SYBR green (Applied Biosciences) assays in ABI7900 real-time PCR system. GAPDH was used as housekeeping gene for normalizations. Relative quantification of expression was calculated using the $2^{-\Delta\Delta CT}$ method [23]. Three independent biological replicates were analyzed in duplicate. All primers were subjected to a quality control to assure that each primer set (forward and reverse) generates a specific PCR product. Primer information is provided in Supplementary Table 1.

In Silico Prediction Analysis of miRNAs

Three different bioinformatics algorithms, miRanda, TargetScan, and PicTar, were used to identify miRNAs predicted to target a set of genes that were significantly downregulated by PE (Suppl. Table 2). The application of a single miRNA target prediction program results in high levels of false positive and false negative discovery rates [24]. However, a combination of two or more programs increases the rate of known target prediction up to 72.6% or 100% for evolutionary conserved targets [24]. The miRanda program predicts miRNA targets by taking into consideration maximum weightage of sequence complementarity to the bases comprising of seed region [25,26]. It also calculates hybridization energy between miRNA–mRNA using RNAFold. The TargetScan program finds the simple 7-nucleotide perfect seed sequence match between the mRNA target region and 5′ end of miRNA [27]. TargetScan further extends the sequence match by allowing G:U wobble pairing and uses hybridization energy (RNAFold) to calculate thermodynamic free energy for binding the remaining base pairing portion. The PicTar program matches perfect 7-mer starting at position 1 or 2 at the 5′ end of the miRNA calculates hybridization energy and discards unstable duplexes [28].

qRT-PCR for miRNAs

Total RNA was extracted using Trizol reagent according to the manufacturer's recommendations (Life Technologies, Ambion). The total RNA preparations that include miRNAs were analyzed for purity using NanoDrop 1000 Spectrophotometer (Thermo Fisher Scientific). miRNA cDNA was synthesized from 1 μg of purified total RNA using qScript miRNA cDNA synthesis kit (Quanta Biosciences, Gaithersburg, MD) and qRT-PCR was performed in 20 μL reaction volume containing 4 μL template

cDNA and 16 μL of reaction mix containing PerfeCTa SYBR green master mix, 10 μM PerfeCTa Universal PCR primer and 10 μM PerfeCTa miRNA assay primer in ABI7900 real-time PCR system. The samples were initially heated at 95°C for 2 min followed by 40 cycles of 95°C for 5 s and 60°C for 30 s. The results were normalized to RNU6B expression and quantified using $2^{-\Delta\Delta CT}$ method. Three independent biological replicates were analyzed in duplicate. Primer information is provided in Supplementary Table 3.

Statistical Analysis

Results were expressed as a mean ± standard error of the mean. Two-way ANOVA was used to estimate the overall significance using Student's *t*-test, *P* values below 0.05 were considered statistically significant.

RESULTS

Growth Inhibition by PE

The effects of various doses of PE treatment on MCF-7 cell growth are shown in Figure 1. Treatment with 0–100 μg/mL of PE significantly inhibited MCF-7 cell growth in a dose- and time-dependent manner as measured by acid phosphatase assay (Figure 1A) and crystal violet assay (Figure 1B). Both assay measurements showed similar effects at all the doses and time points. A dose of 20 μg/mL inhibited cell growth by approximately 30% and 35% at 72 and 96 h, respectively, whereas 50 μg/mL of PE inhibited cell growth by about 50% and 80% at 72 and 96 h, respectively, compared to untreated controls. Cell numbers remained similar throughout the treatment period at an exposure dose of 50 μg/mL, indicating the significant inhibition of cell growth. Given that PE is standardized to ~40% punicalagin and 3.4% free ellagic acid, 50 μg/mL of PE is equivalent to ~18.44 μM punicalagin and ~5.62 μM free ellagic acid, whereas the relative proportions of other ellagitannins are unknown.

We also examined the effect of PE pretreatment. Cells maintained in PE-free medium after PE pretreatment showed about threefold reduction or 48 h delay in cell growth in comparison to their respective controls (Figure 1C). This suggested that PE-gene interactions established during treatment were responsible for the sustained growth arrest.

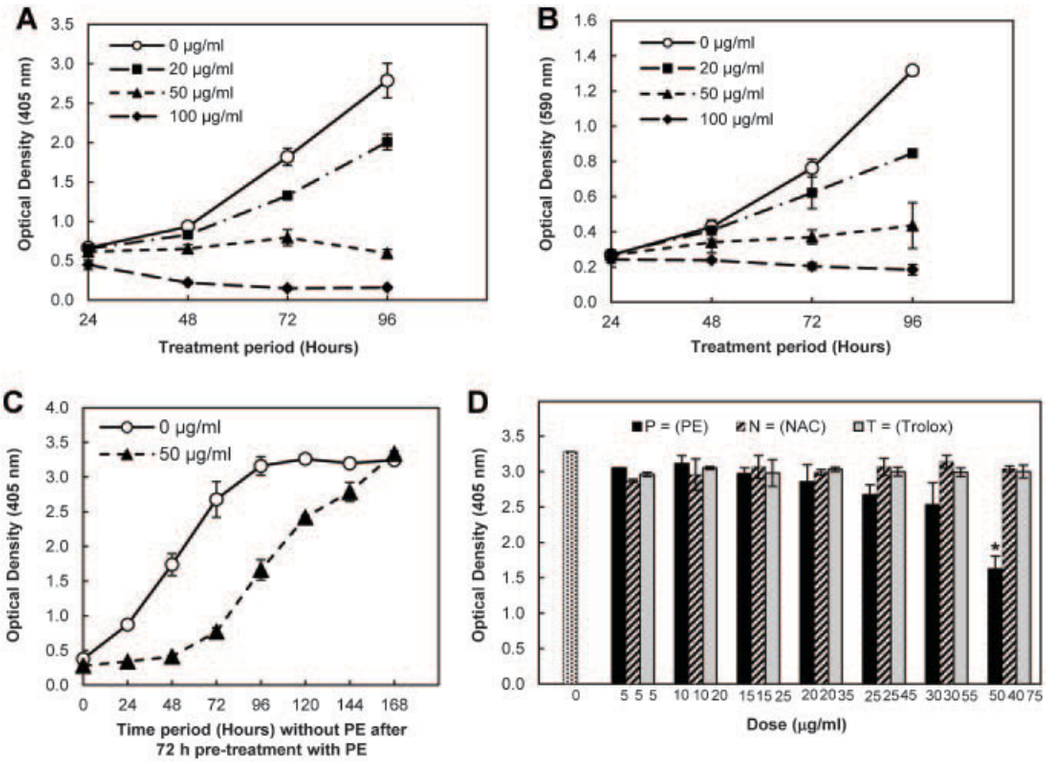

Figure 1. Treatment effects on MCF-7 cell growth. Effect of PE treatment assessed by (A) acid phosphatase assay and (B) crystal violet assay. (C) Effect of PE pretreatment. Cells were pretreated with 50 μg/mL of PE for 72 h followed by incubation in PE-free growth medium. Cell growth was assessed by acid phosphatase assay. (D) Effect of PE, NAC, and Trolox. Solid black, hatched, and gray triplet bars represent doses of PE (P), NAC (N), and Trolox (T) equivalent in terms of TEs. Cell growth was assessed by acid phosphatase assay after 72 h of treatment. $^{*}P < 0.05$, compared to control or equivalent dose of NAC or Trolox.

Comparative Growth Inhibition of PE, NAC, and Trolox

We determined whether cell growth inhibition by PE is due to its antioxidant actions. We used TEAC assay to compare antioxidant capacity of PE, NAC, and Trolox in terms of TEs. For example, antioxidant capacity of 50 μg/mL of PE was found to be equivalent to 40 μg/mL (220 μM) of NAC and 75 μg/mL (280 μM) of Trolox. Growth inhibition of equivalent doses of PE, NAC, and Trolox is shown in Figure 1D. In agreement with the results in Figure 1A, PE inhibited cell growth in a dose-dependent manner. However, NAC or Trolox at doses containing equivalent antioxidant capacity as PE did not inhibit cell growth. This indicated that the growth-inhibitory action of PE cannot solely be attributed to its antioxidant capacity. NAC is known to inhibit cancer cell growth but at concentrations that are three orders of magnitude higher (tens of mM) than used in our study [29–31] while cytostatic doses of Trolox have not been established.

Cell Cycle Analysis

Consistent with the cell viability assay results flow cytometric analysis showed continuous cell growth inhibition with 50 μg/mL of PE throughout the 72 h treatment period. Figure 2 shows flow cytometry results for 0 and 50 μg/mL of PE treatment for 48 h. PE treated cells accumulated in G_2 phase possibly due to G_2/M cell cycle arrest and also underwent apoptosis (Figure 2). The degree of cell cycle inhibition was similar at 24 and 72 h (data not shown). These results indicate that interference with cell cycle regulation pathways may be one of the mechanisms of cell growth inhibition by PE.

Genome-Wide Effects of PE on MCF-7 Transcriptome

A total of 903 differentially expressed gene entities (1.5-fold cutoff, $P < 0.05$) were identified in cells treated with 50 μg/mL of PE for 72 h, where 398 genes were downregulated and 505 genes were upregulated (Figure 3). DAVID functional annotation analysis, performed to highlight the most relevant GO-term enrichment, showed 134 enriched terms associated with downregulated genes and 264 enriched terms associated with upregulated genes. Top over-represented cellular processes sorted by Score, −log(*P*-value), are shown in Figure 3B and C. Twenty-four differentially expressed genes (13 downregulated and 11 upregulated) were selected for qRT-PCR validation based on genes classified for cancer-related enriched GO-terms (mitosis, DNA replication, DNA repair, chromosomal organization, chromosomal segregation, regulation of apoptosis, regulation of cell proliferation) and those that displayed the greatest extreme in differential expression (independent of the GO-term, based on lowest *P*-values). The differential gene expression of most of these genes was confirmed by qRT-PCR (Figure 4). We focused on cellular processes that may explain growth inhibitory and proapoptotic effects of PE, such as DNA damage response, DNA repair and cell cycle control. DNA damage response and repair genes including *MRE11*, *RAD50*, *NBS1*, *RAD51*, *BRCA1*, *BRCA2*, *BRCC3*, and *MSH6* that were downregulated in microarrays, showed a reduction in mRNA levels over a period of 72 h, where the greatest reduction was observed at 72 h (Figure 4A). The importance of these genes is underscored by the fact that the proteins encoded by *RAD50*, *NBS*, and *MRE11* form the MRE11–RAD50–NBS1 (MRN) complex, which acts as double strand break (DSB) sensor, maintains genome stability during replication, promotes homologous recombination (HR) repair, activates ATM for recruitment to damaged DNA and is essential for cell viability [32]. RAD51 is a central player in most HR repair events [33]. BRCA1 has a

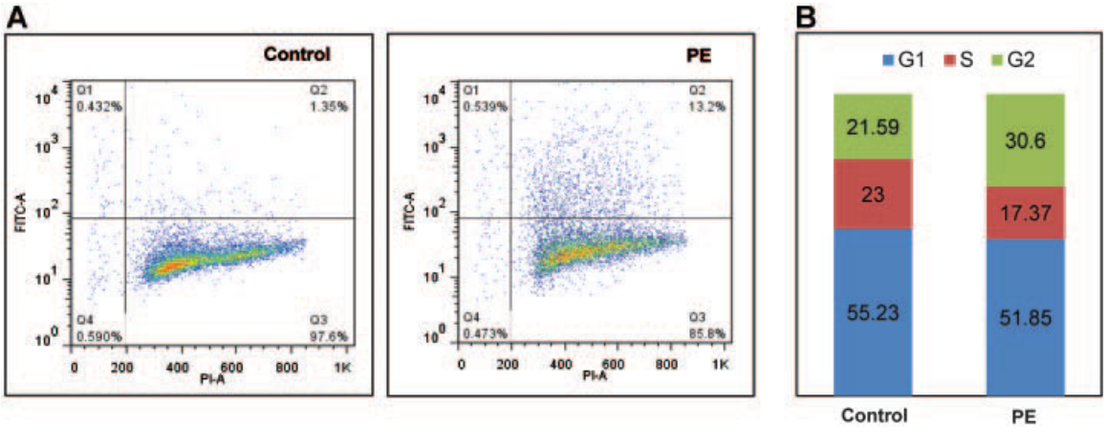

Figure 2. Flow cytometric analysis of PE treatment in MCF-7 cells. (A) Scatter plots of flow cytometric analysis. Live cells are shown in bottom right quadrant (Q3) and apoptotic cells are shown in upper right quadrant (Q2). Numbers at the corner of Q2 indicates the percentage of apoptotic cells. (B) Cell cycle phase distribution. One representative experiment of three is shown.

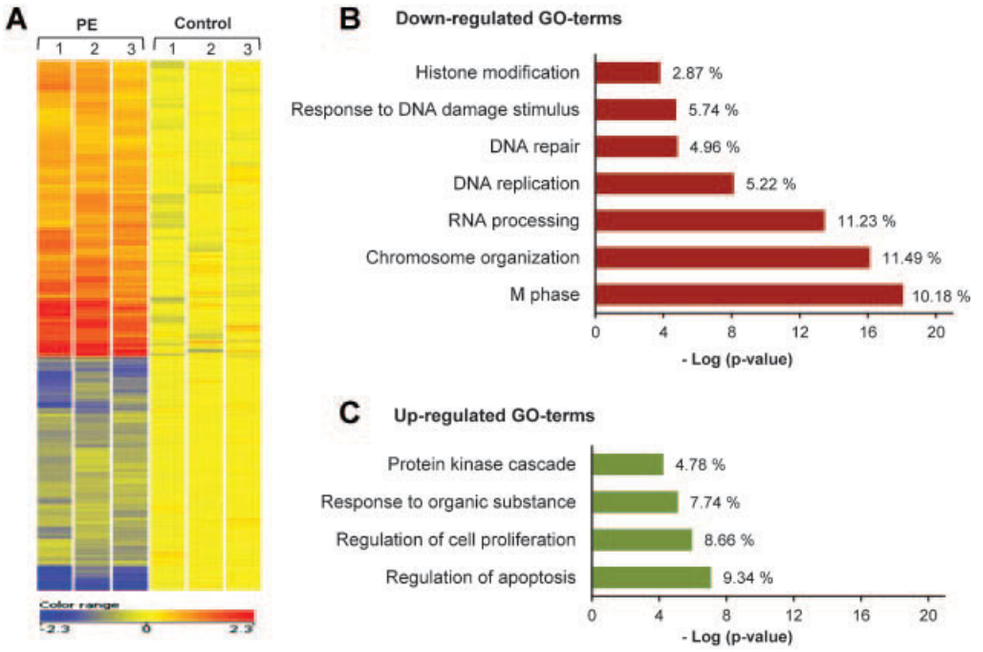

Figure 3. Microarray analysis of PE treatment in MCF-7 cells. (A) Heat map showing relative gene expression changes after PE treatment. (B) Highly enriched GO-terms significantly downregulated after PE treatment. (C) Highly enriched GO-terms significantly upregulated after PE treatment. Percentages to the right of the bars represent a percentage of total genes altered in the respective GO.

pleotropic function in DNA damage signaling and repair [34]. Importantly, most of downregulated DNA repair genes including *MRE11*, *RAD50*, *NBS1*, *RAD51*, *BRCA1*, *BRCA2*, and *BRCC3* are involved HR-mediated repair, suggesting that PE specifically targets HR and thereby sensitizes cells to DSBs, cell cycle arrest and apoptosis.

Figure 4B shows qRT-PCR validation of the genes that play a role in cell cycle control in addition to other processes and include *MCM6*, *SLK*, *PLK1*, *GADD45A*, *CDKN1A*, *E2F2*, and *CCNA2*. All the genes with the exception of p53 downstream targets *GADD45A* (growth arrest and DNA-damage-inducible) and *CDKN1A* (p21) exhibited the pattern observed in microarrays. *GADD45A* and *CDKN1A* were found to be upregulated in microarrays (by threefold) but did not show significant upregulation in qRT-PCR after 24, 48, and/or 72 h suggesting that the PE-induced cell cycle arrest is independent of GADD45A and CDKN1A and perhaps p53.

In addition, we performed qRT-PCR for some of the known PE targets, such as JNK-2, AKT, and PI3K genes (Figure 4C), which did not appear to be significantly altered in our microarray analysis, but were indicated as potential upstream players of DNA repair and cell cycle control by Ingenuity Pathway Analysis (IPA). The observed fold-change reduction in mRNA levels of these genes is consistent with the reduction in their protein levels and/or activity reported in other studies [35,36]. IPA identified a highly significant network associated with DNA repair and M-phase GO-terms. The network involves the genes that were differentially expressed by PE treatment and thus provides a valuable model for understanding the complex mechanism of PE mediated growth inhibition (Figure 5).

γ-H2AX Foci Formation in PE Treated Cells

Because PE downregulated important DSB response and repair genes, we determined the frequency of DSBs by immunofluorescence of γ-H2AX (Figure 6A). γ-H2AX foci form rapidly after DSB formation and resolve following repair and thus represent a sensitive measure of DSB formation and repair [37]. PE treatment resulted in an elevated frequency of γ-H2AX foci with the highest increase (∼2-fold) at 72 h (Figure 6B).

Effects of PE on miRNA Expression

Binding of short noncoding RNA, miRNA, to the target mRNA can lead to mRNA degradation or translational repression. Dietary compounds were shown to modify miRNAs involved in a variety of biological processes but whether PE can regulate miRNAs involved in DNA repair is unknown [38]. We used three different bioinformatics algorithms, miRanda, TargetScan, and PicTar, to identify miRNAs predicted to target the mRNA of *MRE11A*,

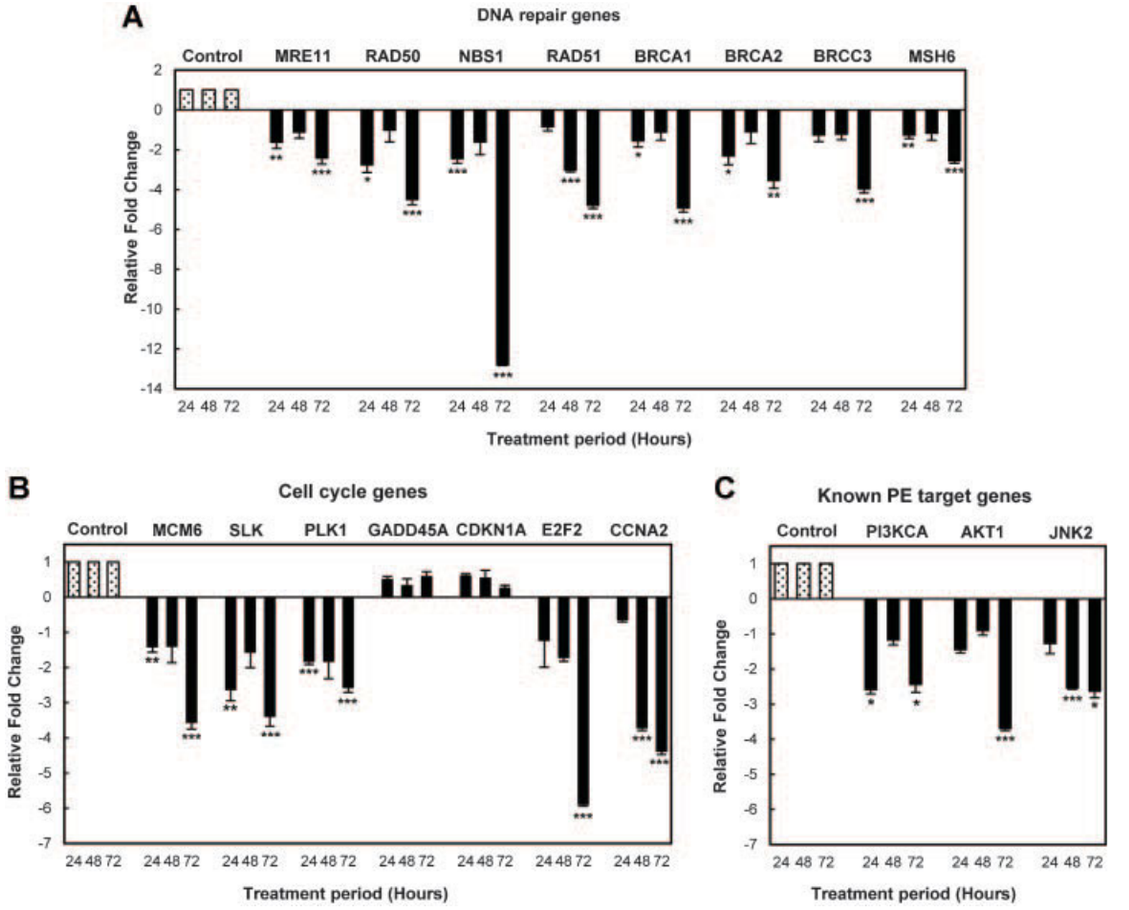

Figure 4. Changes in gene expression levels after PE treatment. (A) DNA repair genes. (B) Cell cycle control genes. (C) Known PE targets. Relative fold-change was determined by qRT-PCR, $^{*}P < 0.05$, $^{**}P < 0.01$, $^{***}P < 0.001$, compared to respective control.

RAD50, *NBS1*, *RAD51*, *BRCA1*, and *BRCA2* genes (Suppl. Table 2) and performed qRT-PCR on miRNAs that were common in two or three algorithms and showed the highest prediction score. Screening for common miRNAs in two or more bioinformatics programs increases the rate of known target prediction to 72.6% and up to 100% for evolutionary conserved targets [24]. Comparative analysis predicted miR-183 to have a seed binding site in the 3′Untranlated Region (3′UTR) of *RAD50* (predicted by all three algorithms) and miR-132 to have seed binding sites in the 3′UTR of *BRCA1* (predicted by two of three algorithms). The 3′UTR of *RAD50* contains only a single seed binding site for miR-183 that is conserved across ten vertebrate species (TargetScan PCT score 0.37), which strongly increases the probability that *RAD50* is a target of miR-183. We also chose to examine miR-24, which has seedless binding sites in the 3′UTR of genes downregulated in our microarray including *BRCA1*, *E2F2*, and *CCNA2*. Importantly, *BRCA1*, *E2F2*, and *CCNA2* genes have been validated experimentally by luciferase assay as being direct targets of miR-24 [39].

PE treatment resulted in a significant upregulation of miR-183 and miR-24 but not miR-132 (Figure 7). Increased miR-183 levels correlated inversely with mRNA levels of *RAD50* (refer to Figure 4A) suggesting a possible communication between miR-183 and *RAD50*. Similarly, there was an inverse correlation between miR-24 and mRNA levels of *BRCA1*, *E2F2*, and *CCNA2* (Figure 4A and B). In summary, these data are suggestive that PE may upregulate miRNAs involved in DNA repair and cell cycle control but further experimentation is needed.

DISCUSSION

The observations in the present study demonstrate cellular and molecular actions of PE beyond antioxidation in MCF-7 cells including evidence of downregulation of DNA repair. While earlier studies have reported growth inhibitory, proapoptotic, and

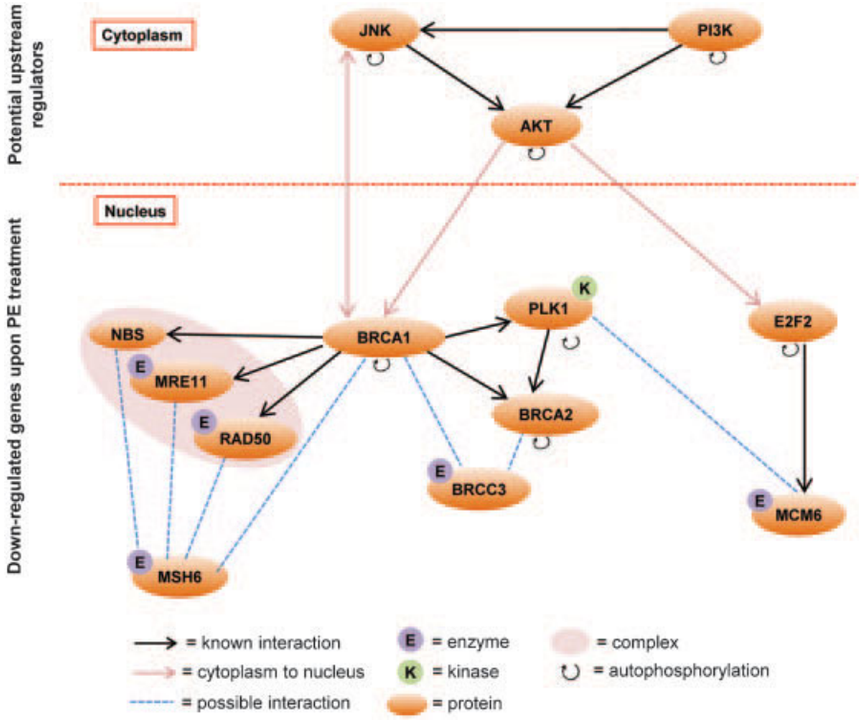

Figure 5. Ingenuity Pathway Analysis of significantly downregulated genes after PE treatment. Interactions between cell cycle control and DNA repair genes and possible upstream regulators are shown.

antiinvasive properties of PE in different cancer cell lines [4,5,7,9,12], this is the first study to demonstrate that PE may affect DNA repair pathway required for the survival of cancer cells.

Consistent with earlier reports, our study confirmed that PE treatment inhibited cancer cell growth in a dose- and time-dependent manner, as assessed by two independent cell growth and viability assays. Growth inhibition was associated with the G_2/M cell cycle arrest and the induction of apoptosis. Secondly, PE pretreatment significantly delayed cell growth. This finding may be of clinical relevance and suggests that intermittent exposure to PE dietary supplements might be effective without compromising anticancer activities, which may be deemed as a more feasible dietary approach. Thirdly,

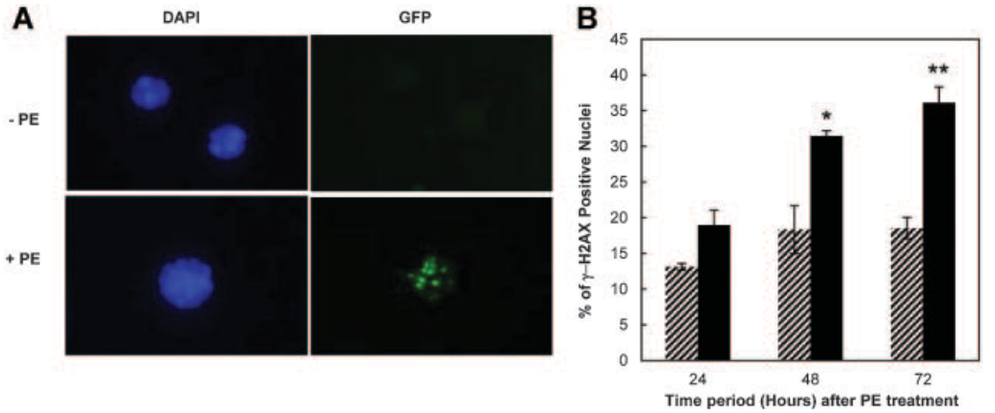

Figure 6. Effect of PE on γ-H2AX foci formation. (A) Representative images of γ-H2AX foci formation after PE treatment. DAPI staining shows cellular nuclei and GFP staining indicates the presence of γ-H2AX foci (B) Percentage of positive nuclei for γ-H2AX foci formation. Hatched bars and solid bars represent untreated cells and cells treated with 50 μg/mL of PE, respectively, $^{*}P < 0.05$, $^{**}P < 0.01$, compared to respective control.

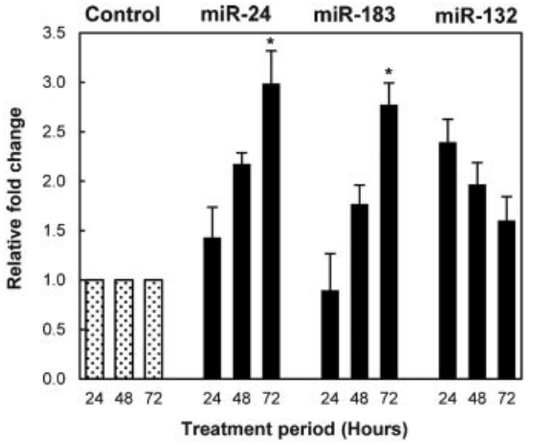

Figure 7. Changes in miRNA expression levels after PE treatment. Relative fold-change was determined by qRT-PCR, $^{*}P < 0.05$, compared to respective control. miR-24 targets *BRCA1*, *E2F2*, and *CCNA2*, miR-183 is predicted to target *RAD50* and miR-132 is predicted to target *BRCA1*.

comparative growth inhibition assessment of PE, NAC, and Trolox suggests that the growth inhibition by PE is not solely attributed to its high antioxidant potential. This was a strong rationale for investigation of other possible mechanisms of action, for which we employed Affymetrix microarrays. Microarray analysis showed that PE treatment significantly modulated over 900 genes. The most enriched GO-terms among downregulated genes included mitosis, chromosomal organization, RNA processing, DNA replication, DNA damage response, and DNA repair, whereas the most enriched GO-terms among upregulated genes included regulation of apoptosis and regulation of cell proliferation. Although many of these cellular processes may control cell growth and death, this study links for the first time PE exposure and downregulation of DNA repair genes.

Of particular interest, most of the DNA repair genes that were downregulated by PE are involved in HR-mediated repair [33,40,41]. For example, the MRN complex together with CtIP facilitates 5′–3′ resection of DSB ends required for initiation of HR. BRCA1 interacts with both MRN and CtIP and may be involved in end resection, although BRCA1 has pleiotropic functions and its exact role in HR is difficult to dissect. On the contrary, BRCA2 is predominantly involved in HR. The 3′-single-stranded DNA overhang generated during end resection is bound to replication protein A (RPA), which is required for subsequent recruitment of RAD51. BRCA2 displaces RPA and facilitates loading of RAD51 onto single-stranded DNA. RAD51 forms the nucleoprotein filament that catalyzes strand exchange during which single-stranded DNA invades homologous duplex DNA forming a displacement loop (D-loop), required for subsequent HR reactions. BRCA2 binds RAD51 through interactions with a series of eight short conserved repeats stimulating nucleoprotein filament formation. Also, BRCA2 itself binds to single-stranded DNA. Both BRCA1 and BRCA2 deficient cells are defective for HR. The role of BRCC3 in HR is uncertain. However, it directly interacts with BRCA1 and is required for ionizing radiation-induced BRCA1 phosphorylation and nuclear foci formation [42]. Importantly, BRCC3 is aberrantly expressed in the majority of breast cancer cell lines and in invasive ductal carcinomas, suggesting a potential role in breast cancer [43]. MSH6, a mismatch repair protein, has also been linked to HR. MSH6 has been shown to co-localize with BLM, p53, and RAD51 in hydroxyurea-induced RAD51 nuclear foci that may correspond to the sites of presumed stalled DNA replication forks, which are subject to HR repair [44]. Altogether, this illustrates that PE may influence multiple steps of the HR reaction.

HR pathway is only active during the S and G_2 phases of the cell cycle since the sister chromatid, a preferential substrate for HR, is present only after DNA replication [33,40,45]. It is possible that HR could use homologous chromosomes for DSB repair in the G_1 phase but this would result in genome rearrangements. To avert this scenario, HR is controlled not only by DNA damage response signaling pathways but also cell cycle regulators as well as chromatin remodeling factors [45]. In our study, PE-treated cells were arrested in G_2/M, which provides a time and substrate for HR to occur. However, we also found that important chromatin remodeling genes (RUVBL1/Tip49, RSF1, and RNF20) were downregulated by PE.

As noted above, HR occurs predominantly in replicating cells, while an alternative DSB repair pathway, nonhomologous end joining (NHEJ), prevails in quiescent and postmitotic cells. Thus, it is reasonable to assume that HR is essential for the maintenance and viability of cancer cells but not normal quiescent cells. To support this notion, a study using *Rad50* conditional knock-out mice showed that depletion of Rad50 in cultured cells caused extensive DNA damage and death within 3–5 d. On the contrary, Rad50 was dispensable for viability of quiescent and postmitotic tissues [46]. These findings support the idea that HR is not essential in nondividing cells. In agreement with this, HR was found to be spontaneously increased in breast cancer cells while NHEJ was not, as shown by plasmid reporter assays measuring DSB repair by HR and/or NHEJ [47]. In addition to DSB repair, HR also repairs stalled and collapsed replication forks (i.e., replication-associated lesions). There is experimental evidence suggesting that DSBs are not the primary substrate for HR in mitotic cells, whereas most spontaneous HR in mitotic cells is induced by stalled replication forks [45]. Both unrepaired DSBs and

replication-associated lesions will ultimately culminate in cell death. Our findings that PE downregulated the MRN complex subunits, *MRE11*, *RAD50*, *NBS1*, and *RAD51*, *BRCA1*, *BRCA2*, *BRCC3*, and *MSH6*, and increased DSBs, suggest that these may be the possible causes for reduced cancer cell survival following PE treatment. The mechanism of downregulation of DNA repair genes by PE is currently unclear. Our study suggests that miRNAs may be among the possible regulators. We found that PE treatment upregulated miR-183 and miR-24 that are predicted to target RAD50 and BRCA1, respectively. Experimental validation will confirm whether RAD50 is a direct target of miR-183, while BRCA1 has already been validated as miR-24 target [29].

In addition to spontaneous damage, HR is involved in the repair of DNA damage induced by cancer drugs [45,48]. Inhibition of HR amplifies toxic replication-associated DNA lesions that directly result in cell death. HR inhibitors are therefore predicted to be highly efficient at killing tumors. Some newly developed drugs that enhance tumor chemosensitivity and radiosensitivity were shown to target HR (i.e., imatinib, proteasome inhibitors, and histone deacetylase inhibitors) [45,49]. Also, downregulation of HR genes, *BRCA2* and *RAD51*, by interference RNA approach sensitizes cancer cells to chemotherapeutics [50]. Whether PE exclusively downregulates DNA repair genes in cancer cells is unknown. Irrespective of this, because the MRN complex is dispensable for the maintenance and viability of postmitotic tissues and HR is only active in replicating cells, it is likely that downregulation of HR in normal tissues would have only a minor effect, provided the NHEJ pathway is intact [46].

Thus, our study showing that PE downregulates HR genes warrants further investigations regarding the use of PE as a nontoxic HR inhibitor available in the form of a whole fruit, fruit juice, or a dietary supplement pill. At present, it is unknown whether PE downregulates HR in vivo. Likewise, it is unclear whether equivalent concentrations of PE ellagitannins (i.e., 18.4 μM punicalagins and 5.6 μM ellagic acid) can be achieved in humans, compounded by the occurrence of different PE metabolites in cultured cells and human tissues. In humans, ellagitannins are hydrolyzed to ellagic acid and further converted by gut microflora to bioavailable urolithins [16,51,52]. Ellagic acid and urolithins undergo conjugation with methyl, glucuronyl, and sulfate groups and are found in plasma and excreted in the urine [16,51–53]. Ellagitannin metabolism, which may be dependent on the intestinal flora or bowel transit time, shows considerable inter-individual variability [16,51,53]. Punicalagin, which is the major ellagitannin present in pomegranate juice and occurs as isomers, was not detected in plasma or urine in humans after consumption of pomegranate juice [51]. Ellagic acid, although poorly absorbed and rapidly metabolized, was detected in human plasma after consumption of a single dose of 8 ounces of pomegranate juice or 1000 mg of PE dietary supplement with a maximum concentration of 0.06 μM at 1 h postingestion [16,53]. In contrast, Cerda et al. [51] reported that ellagic acid was not detected in plasma or urine after daily intake of 1 L of pomegranate juice containing 4.37 g punicalagins over 5 d, but found three ellagitannin metabolites in plasma. The highest concentration of the sum of the three metabolites reached 18.6 μM [51]. Also, Seeram et al. [16] detected increasing concentrations of glucuronyl and sulfate conjugates of urolithin A and urolithin B in plasma samples between 0.5 and 6 h postingestion, with the highest concentration of urolithin A and urolithin B of 0.11 and 0.05 μM, respectively. In the current study, we used 50 μg/mL of PE that is equivalent to 18.4 μM of punicalagins. Because gut flora metabolites are not formed in cell culture, extrapolation of PE concentration in growth medium to human plasma is inaccurate per se. Yet, the fact that ellagitannin metabolites were measured at micromolar concentrations in human plasma after ingestion of pomegranate juice [51] suggests that PE concentration used in this study is a physiologically relevant dose. However, the use of only one cancer cell line is a limitation of this study, which will be addressed in future studies.

In summary, our study suggests that PE targets a specific DNA repair pathway that is critical for cancer cell survival both spontaneously and after drug challenge. This provides a strong rationale for further testing of PE as a nontoxic adjunct to the prevention of breast cancer recurrence through its actions on breast cancer cells. However, further research is needed to demonstrate these effects in animal studies and in tissue samples from women with breast cancer.

ACKNOWLEDGMENTS

The authors would like to thank Dr. JoEllen Welsh, for critical reading of the manuscript, Judy Narvaez for help with flow cytometric analysis, David Frank and Marcy Kuentzel for excellent technical help with the microarray experiments.

REFERENCES

1. Jurenka JS. Therapeutic applications of pomegranate (*Punica granatum* L.): A review. Altern Med Rev 2008;13: 128–144.
2. Lansky EP, Newman RA. *Punica granatum* (pomegranate) and its potential for prevention and treatment of inflammation and cancer. J Ethnopharmacol 2007;109:177–206.
3. Seeram NP, Aviram M, Zhang Y, et al. Comparison of antioxidant potency of commonly consumed polyphenol-rich beverages in the United States. J Agric Food Chem 2008; 56:1415–1422.
4. Syed DN, Afaq F, Mukhtar H. Pomegranate derived products for cancer chemoprevention. Semin Cancer Biol 2007; 17:377–385.

5. Kasimsetty SG, Bialonska D, Reddy MK, Ma G, Khan SI, Ferreira D. Colon cancer chemopreventive activities of pomegranate ellagitannins and urolithins. J Agric Food Chem 2010;58:2180–2187.
6. Wang L, Alcon A, Yuan H, Ho J, Li QJ, Martins-Green M. Cellular and molecular mechanisms of pomegranate juice-induced anti-metastatic effect on prostate cancer cells. Integr Biol (Camb) 2011;3:742–754.
7. Adhami VM, Khan N, Mukhtar H. Cancer chemoprevention by pomegranate: Laboratory and clinical evidence. Nutr Cancer 2009;61:811–815.
8. Seeram NP, Adams LS, Henning SM, et al. In vitro antiproliferative, apoptotic and antioxidant activities of punicalagin, ellagic acid and a total pomegranate tannin extract are enhanced in combination with other polyphenols as found in pomegranate juice. J Nutr Biochem 2005;16:360–367.
9. Mehta R, Lansky EP. Breast cancer chemopreventive properties of pomegranate (*Punica granatum*) fruit extracts in a mouse mammary organ culture. Eur J Cancer Prev 2004; 13:345–348.
10. Kim ND, Mehta R, Yu W, et al. Chemopreventive and adjuvant therapeutic potential of pomegranate (*Punica granatum*) for human breast cancer. Breast Cancer Res Treat 2002;71:203–217.
11. Adams LS, Zhang Y, Seeram NP, Heber D, Chen S. Pomegranate ellagitannin-derived compounds exhibit antiproliferative and antiaromatase activity in breast cancer cells in vitro. Cancer Prev Res (Phila) 2010;3:108–113.
12. Khan GN, Gorin MA, Rosenthal D, et al. Pomegranate fruit extract impairs invasion and motility in human breast cancer. Integr Cancer Ther 2009;8:242–253.
13. Dai Z, Nair V, Khan M, Ciolino HP. Pomegranate extract inhibits the proliferation and viability of MMTV-Wnt-1 mouse mammary cancer stem cells in vitro. Oncol Rep 2010;24:1087–1091.
14. Thomas HV, Reeves GK, Key TJ. Endogenous estrogen and postmenopausal breast cancer: A quantitative review. Cancer Causes Control 1997;8:922–928.
15. Patel C, Dadhaniya P, Hingorani L, Soni MG. Safety assessment of pomegranate fruit extract: Acute and subchronic toxicity studies. Food Chem Toxicol 2008;46:2728–2735.
16. Seeram NP, Henning SM, Zhang Y, Suchard M, Li Z, Heber D. Pomegranate juice ellagitannin metabolites are present in human plasma and some persist in urine for up to 48 hours. J Nutr 2006;136:2481–2485.
17. Wisman KN, Perkins AA, Jeffers MD, Hagerman AE. Accurate assessment of the bioactivities of redox-active polyphenolics in cell culture. J Agric Food Chem 2008;56: 7831–7837.
18. Gillies RJ, Didier N, Denton M. Determination of cell number in monolayer cultures. Anal Biochem 1986;159:109–113.
19. Yang TT, Sinai P, Kain SR. An acid phosphatase assay for quantifying the growth of adherent and nonadherent cells. Anal Biochem 1996;241:103–108.
20. Prior RL, Hoang H, Gu L, et al. Assays for hydrophilic and lipophilic antioxidant capacity (oxygen radical absorbance capacity (ORAC(FL))) of plasma and other biological and food samples. J Agric Food Chem 2003;51:3273–3279.
21. Miller NJ, Sampson J, Candeias LP, Bramley PM, Rice-Evans CA. Antioxidant activities of carotenes and xanthophylls. FEBS Lett 1996;384:240–242.
22. Westbrook AM, Wei B, Braun J, Schiestl RH. Intestinal mucosal inflammation leads to systemic genotoxicity in mice. Cancer Res 2009;69:4827–4834.
23. Livak KJ, Schmittgen TD. Analysis of relative gene expression data using real-time quantitative PCR and the 2(-Delta Delta C(T)) Method. Methods 2001;25:402–408.
24. Sethupathy P, Megraw M, Hatzigeorgiou AG. A guide through present computational approaches for the identification of mammalian microRNA targets. Nat Methods 2006;3:881–886.
25. Enright AJ, John B, Gaul U, Tuschl T, Sander C, Marks DS. MicroRNA targets in Drosophila. Genome Biol 2003;5:R1.
26. John B, Enright AJ, Aravin A, Tuschl T, Sander C, Marks DS. Human MicroRNA targets. PLoS Biol 2004;2:e363.
27. Lewis BP, Burge CB, Bartel DP. Conserved seed pairing, often flanked by adenosines, indicates that thousands of human genes are microRNA targets. Cell 2005;120:15–20.
28. Krek A, Grun D, Poy MN, et al. Combinatorial microRNA target predictions. Nat Genet 2005;37:495–500.
29. Yuan J, Chen J. MRE11-RAD50-NBS1 complex dictates DNA repair independent of H2AX. J Biol Chem 2010;285: 1097–1104.
30. Kusano C, Takao S, Noma H, et al. N-acetyl cysteine inhibits cell cycle progression in pancreatic carcinoma cells. Hum Cell 2000;13:213–220.
31. Lee YJ, Lee DM, Lee CH, et al. Suppression of human prostate cancer PC-3 cell growth by N-acetylcysteine involves over-expression of Cyr61. Toxicol In Vitro 2011;25:199–205.
32. D'Amours D, Jackson SP. The Mre11 complex: At the crossroads of dna repair and checkpoint signalling. Nat Rev Mol Cell Biol 2002;3:317–327.
33. Helleday T, Lo J, van Gent DC, Engelward BP. DNA double-strand break repair: From mechanistic understanding to cancer treatment. DNA Repair (Amst) 2007;6:923–935.
34. Roy R, Chun J, Powell SN. BRCA1 and BRCA2: Different roles in a common pathway of genome protection. Nat Rev Cancer 2012;12:68–78.
35. Adams LS, Seeram NP, Aggarwal BB, Takada Y, Sand D, Heber D. Pomegranate juice, total pomegranate ellagitannins, and punicalagin suppress inflammatory cell signaling in colon cancer cells. J Agric Food Chem 2006;54:980–985.
36. Rasheed Z, Akhtar N, Anbazhagan AN, Ramamurthy S, Shukla M, Haqqi TM. Polyphenol-rich pomegranate fruit extract (POMx) suppresses PMACI-induced expression of pro-inflammatory cytokines by inhibiting the activation of MAP Kinases and NF-kappaB in human KU812 cells. J Inflamm 2009;6:1.
37. Pilch DR, Sedelnikova OA, Redon C, Celeste A, Nussenzweig A, Bonner WM. Characteristics of gamma-H2AX foci at DNA double-strand breaks sites. Biochem Cell Biol 2003;81: 123–129.
38. Karius T, Schnekenburger M, Dicato M, Diederich M. MicroRNAs in cancer management and their modulation by dietary agents. Biochem Pharmacol 2012;83:1591–1601.
39. Lal A, Navarro F, Maher CA, et al. miR-24 Inhibits cell proliferation by targeting E2F2, MYC, and other cell-cycle genes via binding to ''seedless'' 3'UTR microRNA recognition elements. Mol Cell 2009;35:610–625.
40. Kass EM, Jasin M. Collaboration and competition between DNA double-strand break repair pathways. FEBS Lett 2010; 584:3703–3708.
41. Reliene R, Bishop AJ, Schiestl RH. Involvement of homologous recombination in carcinogenesis. Adv Genet 2007; 58:67–87.
42. Chen X, Arciero CA, Wang C, Broccoli D, Godwin AK. BRCC36 is essential for ionizing radiation-induced BRCA1 phosphorylation and nuclear foci formation. Cancer Res 2006;66:5039–5046.
43. Dong Y, Hakimi MA, Chen X, et al. Regulation of BRCC, a holoenzyme complex containing BRCA1 and BRCA2, by a signalosome-like subunit and its role in DNA repair. Mol Cell 2003;12:1087–1099.
44. Obad S, Brunnstrom H, Vallon-Christersson J, Borg A, Drott K, Gullberg U. Staf50 is a novel p53 target gene conferring reduced clonogenic growth of leukemic U-937 cells. Oncogene 2004;23:4050–4059.
45. Helleday T. Homologous recombination in cancer development, treatment and development of drug resistance. Carcinogenesis 2010;31:955–960.
46. Adelman CA, De S, Petrini JH. Rad50 is dispensable for the maintenance and viability of postmitotic tissues. Mol Cell Biol 2009;29:483–492.

47. Mao Z, Jiang Y, Liu X, Seluanov A, Gorbunova V. DNA repair by homologous recombination, but not by nonhomologous end joining, is elevated in breast cancer cells. Neoplasia 2009;11:683–691.
48. Helleday T, Petermann E, Lundin C, Hodgson B, Sharma RA. DNA repair pathways as targets for cancer therapy. Nat Rev Cancer 2008;8:193–204.
49. Choudhury A, Zhao H, Jalali F, et al. Targeting homologous recombination using imatinib results in enhanced tumor cell chemosensitivity and radiosensitivity. Mol Cancer Ther 2009;8:203–213.
50. Quiros S, Roos WP, Kaina B. Rad51 and BRCA2—New molecular targets for sensitizing glioma cells to alkylating anticancer drugs. PLoS ONE 2011;6:e27183.
51. Cerda B, Espin JC, Parra S, Martinez P, Tomas-Barberan FA. The potent in vitro antioxidant ellagitannins from pomegranate juice are metabolised into bioavailable but poor antioxidant hydroxy-6H-dibenzopyran-6-one derivatives by the colonic microflora of healthy humans. Eur J Nutr 2004; 43:205–220.
52. Cerda B, Tomas-Barberan FA, Espin JC. Metabolism of antioxidant and chemopreventive ellagitannins from strawberries, raspberries, walnuts, and oak-aged wine in humans: Identification of biomarkers and individual variability. J Agric Food Chem 2005;53:227–235.
53. Seeram NP, Zhang Y, McKeever R, et al. Pomegranate juice and extracts provide similar levels of plasma and urinary ellagitannin metabolites in human subjects. J Med Food 2008;11:390–394.